ELSEVIER

Polymer 40 (1999) 3855–3865

polymer

Annealing effect on the ferroelectric phase transition behavior and domain structure of vinylidene fluoride (VDF)–trifluoroethylene copolymers: a comparison between uniaxially oriented VDF 73 and 65% copolymers

Rieko Tanaka, Kohji Tashiro*, Masamichi Kobayashi

Department of Macromolecular Science, Graduate School of Science, Osaka University, Toyonaka, Osaka 560-0043, Japan

Received 12 May 1998; received in revised form 14 August 1998; accepted 24 August 1998

Abstract

The structure and ferroelectric phase transition behavior were investigated for heat-treated samples of vinylidene fluoride–trifluoroethylene (VDF–TrFE) copolymers with 73 and 65% VDF molar contents. The temperature of the transition from the ferroelectric to the paraelectric phases increased when the samples were annealed in the temperature region of the above phase transition. The domain size, evaluated from the integrated width of the X-ray reflections, also increased drastically at these annealing temperatures. As the annealing temperature increased above the transition point, the resulting sample showed a reduction of the transition temperature. In this case, the domain size decreased slightly and the trans sequential length in the crystalline domain decreased, corresponding to structural disorder due to the invasion of gauche bonds into the trans zigzag chains. In the case of the 65% VDF sample, annealing in the phase transition temperature region resulted in a tilting phenomenon of chains in the crystalline region, but this phenomenon was not detected for the 73% VDF sample.

Keywords: Vinylidene fluoride–trifluoroethylene copolymers; Phase transition; X-ray diffraction

1. Introduction

1.1. Characteristic features of phase transitions

Vinylidene fluoride–trifluoroethylene (VDF–TrFE) copolymers have attracted much interest since their unique ferroelectric phase transition was discovered for the first time in the synthetic polymers [1–6]. This ferroelectric phase transition is unique in that the chain conformation changes drastically between the trans and the gauche forms at the so-called Curie transition temperature (T_c) [7–14]. This conformational change is accompanied by a rotational motion of the chains around the chain axes, resulting in the disappearance of the dipole moment of the crystal above T_c. Such a large conformational change is characteristic of polymers in which the monomer units or the polar CH_2CF_2 dipoles are connected strongly through covalent bonding, and is quite different from the structural change observed at the ferroelectric phase transition of low-molecular-weight compounds in which small ionic groups rotate or translate slightly.

The structural change occurring at the ferroelectric phase transition of the VDF–TrFE copolymers has been studied by X-ray diffraction and infrared and Raman spectroscopic methods [7–15]. As shown in Fig. 1(a) and 1(b), two types of ferroelectric phases, the low-temperature (LT) and the cooled (CL) phases, exist depending on the VDF content of the copolymers as well as on the sample preparation conditions. The LT phase consists of a parallel arrangement of CF_2 dipoles of the planar-zigzag all-trans chains as is likely in the case of PVDF form I, while in the CL phase the long trans segments are connected along the chain axis by irregular trans–gauche linkages to form a kind of superstructure. The CL phase is transformed to the LT phase by the application of a tensile force along the chain axis or an electric field along the polar axis. Above T_c, these phases transform into the high-temperature (HT) phase, with contracted chains consisting of a statistical array of TT, TG, and T$\bar{G}$ rotational isomers. Through trans–gauche conformational exchange, the molecular chains rotate violently in the paraelectric HT phase [16–22], resulting in the non-polar unit cell structure of hexagonal packing (Fig. 1(c)).

Ohigashi and co-workers [23] and Tashiro et al. [24] proposed the concept of domain structure in the crystallites of the copolymers on the basis of experimental data relating

* Corresponding author.

0032-3861/99/$ - see front matter
PII: S0032-3861(98)00609-0

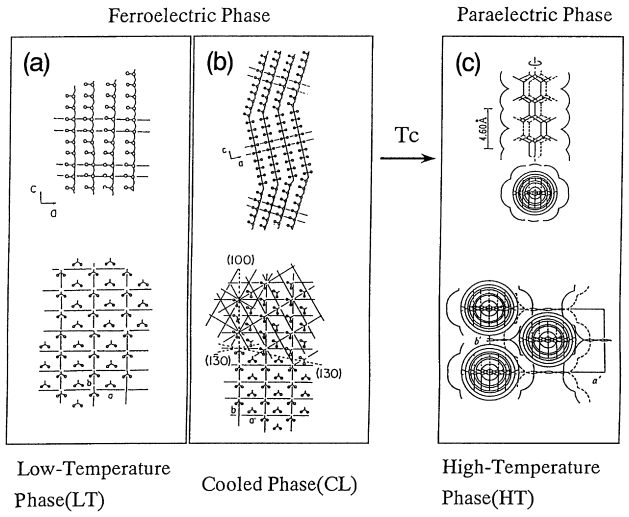

Fig. 1. Crystal structures of (a) the low-temperature phase, (b) the cooled phase and (c) the high-temperature phase of VDF–TrFE copolymer [4].

to the temperature dependence of the X-ray diffraction pattern. As the temperature increases and the LT phase changes into the HT phase, the X-ray profile changes markedly: the reflection of the LT phase is, in general, broad and the reflection of the HT phase generated at the early stage of transition is also relatively broad and rather close to that of the LT phase. The reflection width of the HT phase becomes markedly sharper as the transition proceeds further at higher temperature, while the half-width of the reflection of the LT phase remains broad and almost constant during the transition. These observations suggest the existence of domain structure and its growth during the phase transition [24]. The crystallite of the LT phase is assumed to have a multi-domain structure where domains of size approximately 100 Å in the lateral direction, as evaluated from the X-ray reflection width, congregate with their dipoles oriented in different directions to form a large crystallite, as illustrated in Fig. 2. As the temperature increases and approaches the T_c, the HT phase begins to appear randomly in some of the domains, and the domain size of the HT phase reflects directly that of the LT phase, giving a reflection width close to that of the LT phase. As the temperature increases further, the number of domains in the HT phase increases and these domains are fused together into a large single domain because a large-amplitude rotation of the chains makes each domain non-polar and so the boundary between the domains becomes unambiguous, these domains fusing into one large domain. The large size of the domain thus-created is reflected in the sharpness of the X-ray reflection.

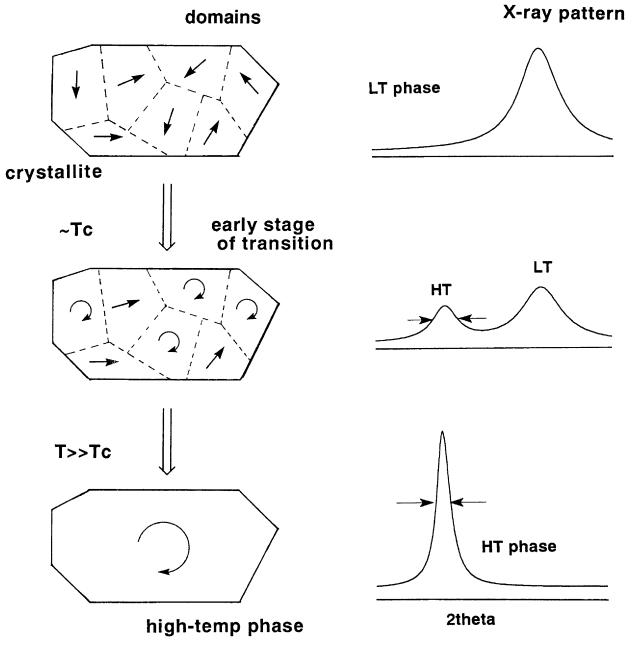

Fig. 2. Illustration of the growth of the domain size during the phase transition from the LT to HT phases, and the corresponding change in the X-ray reflection profiles predicted for each structure [24].

1.2. Factors affecting the transition behavior

The above-mentioned transition behavior is affected by many factors. For example, the transition behavior changes depending upon the VDF content of the copolymers [4,10–13]. For copolymers with a VDF content higher than 70 mol%, the transition occurs almost reversibly and discontinuously in a thermodynamically first-order fashion between the regular LT phase and the HT phase. For samples with VDF 70–60%, the crystalline phase, obtained by heat treatment above the T_c, is a mixture of the LT and CL phases at room temperature, and apparently complicated transitions are observed, as will be clarified in a later section. For copolymers with a VDF content of 0–50%, a transition occurs apparently continuously over a wide temperature range between the CL phase and the HT phase. Heat treatment also markedly affects the T_c as well as the melting point (m.p.) [4,23–27]. For example, Stack and Ting measured DSC thermograms of a series of VDF 70% samples which were prepared by isothermal crystallization at various temperatures, and showed that the T_c changed systematically depending on the crystallization temperature [25]. Kim et al. observed multiple peaks in the DSC thermograms of variously treated samples which were assigned to transitions of the different types of crystalline phases on the basis of infrared spectroscopic data [26]. Ohigashi and co-workers annealed and/or poled VDF 75% copolymer samples at various temperatures, finding the maximal point at a particular annealing temperature [23]. In a previous paper [24], we measured the DSC thermograms of a series of VDF 73% samples which were prepared by annealing melt-quenched samples at various temperatures, and showed that the T_c and m.p. changed systematically depending on the annealing temperature. We evaluated the domain size of these samples by using an X-ray diffraction technique and interpreted the complicated

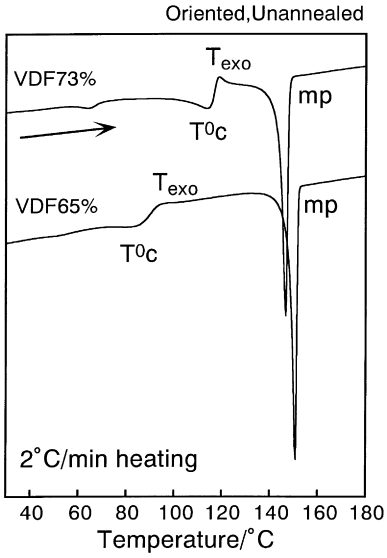

Fig. 3. DSC thermograms measured for uniaxially oriented VDF 73% and 65% samples.

thermal behavior of the VDF 73% sample systematically [24].

The transition behavior of VDF–TrFE copolymers is also affected sensitively by the VDF content and by the condition of the starting crystalline phase, the CL phase or the LT phase. For example, the VDF 65% copolymer consists of a mixture of the LT and CL phases at room temperature after heat treatment above the transition point. Because of the contribution of the CL phase, the transition behavior of the VDF 65% sample is appreciably different from that of the VDF 73% sample, which contains almost purely the LT phase, although the CL phase is also present in a relatively small amount. In order to clarify the relationship between the transition behavior and the crystalline state in more detail, it may be useful to compare the annealing effect on the thermal behavior and the crystalline morphology among copolymer samples of different VDF contents. In this paper, we will anneal VDF 73 and 65% samples at various temperatures and investigate the thermal behavior and structures by using DSC, X-ray diffraction and Raman spectroscopy, and clarify the difference in the characteristic features of the behavior between these two samples based on the domain concept.

2. Experimental

The VDF–TrFE copolymers used here are samples with VDF contents of 73 and 65 mol%. Uniaxially oriented samples were prepared by stretching cast films to around five times the original length at room temperature. These samples were placed in an oil bath at a predetermined temperature (T_a) for 2 h with their ends free from strain, and then quenched rapidly in an ice–water bath in order to avoid an additional annealing effect during slow cooling.

The DSC measurements were performed at a heating rate of 2°C min^{-1} by using a Seiko DSC120 controlled by a SSC5200H disk station. The X-ray diffraction pattern was measured by using a Rigaku RAD-ROC diffractometer with graphite-monochromatized Cu Kα radiation ($\lambda = 1.5418$ Å). The diffraction profiles of the *hk*0 and 00*l* reflections of the uniaxially oriented samples were measured in the reflection and transmission modes, respectively. The X-ray coherent size of the domain D_{hkl} in the direction normal to the *hkl* plane was evaluated on the basis of Scherrer's equation

$$D_{hkl} = \frac{K \cdot \lambda}{\beta \cdot \cos\theta} \tag{1}$$

where 2θ is the diffraction angle, K is a constant of value 1.05, and β is the integrated width corrected for the slit function by using the aluminum reflection as a standard.

$$\beta = \sqrt{\beta_{obs}^2 - \beta_{Al}^2} \tag{2}$$

where β_{obs} is the observed width of a reflection and β_{Al} is the width of the aluminum reflection. X-ray fiber diagrams of the uniaxially oriented samples were measured by using an imaging plate system emploing Mo Kα radiation at $\lambda = 0.71073$ Å (DIP1000 and DIP220, MAC Science Co., Ltd., Japan). The integrated widths of the reflections were evaluated from the X-ray fiber diagram measured by using DIP220 with a cylindrical camera. The equatorial and meridional reflections for the oriented samples were measured by setting their fiber axes parallel and vertical, respectively, to the axis of the cylindrical camera.

Raman spectra of the annealed samples were difficult to obtain because of the disturbance by too strong a fluorescence when a conventional dispersion-type Raman spectrometer was used with a visible laser as the source of the excitation beam. Fourier transform-Raman spectra measured with a near-IR laser beam were found to be quite useful for avoiding this difficulty. The FT-Raman spectra were measured at room temperature by using a Bio-Rad FTS-60A/896 FT-Raman system with an incident light source from an Nd–YAG laser at $\lambda = 1.064$ μm.

3. Results and discussion

3.1. DSC thermograms

Fig. 3 shows DSC thermograms measured during the heating processes for the as-drawn and unannealed VDF 73 and 65% copolymer samples. These curves mainly show four peaks: a small endothermic peak, a larger endothermic peak (T_c^0), an exothermic peak (T_{exo}), and an endothermic melting peak (m.p.). For the VDF 73% copolymer samples, the T_c is higher and the m.p. is lower than those of the VDF 65% samples. These as-drawn samples were annealed at various temperatures and the DSC thermograms were then measured starting from room temperature.

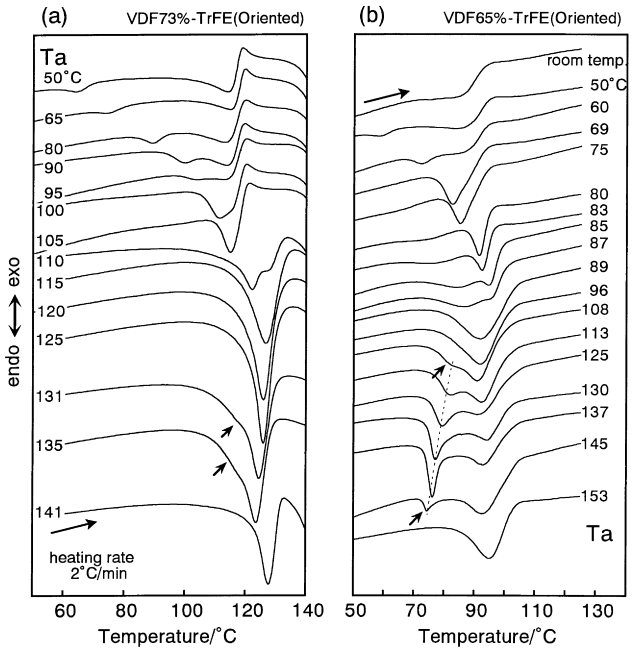

Fig. 4. DSC thermograms measured for uniaxially oriented VDF (a) 73% and (b) 65% samples prepared at various annealing temperatures (T_a).

Fig. 4(a) shows DSC thermograms in the phase transition region measured for the oriented VDF 73% copolymer samples annealed at various temperatures (T_a). As already reported [24], samples annealed at relatively low temperatures (50–100°C) exhibited two endothermic peaks and one exothermic peak in the transition temperature range. As the annealing temperature was increased to 105–125°C, these endothermic peaks gradually shifted toward the higher temperature side and converged into a single peak. When the samples were annealed above the T_c^0 of the unannealed sample (around 120°C), a small endothermic peak began to be detected as a shoulder of the main peak at the lower temperature side, as indicated by an arrow in Fig. 4(a). When the samples were annealed in the m.p. region (approximately 141°C), this shoulder disappeared.

Similar thermal behavior can be also seen in the case of VDF 65% samples as shown in Fig. 4(b). The shoulder detected for the VDF 73% samples annealed at high temperature above T_c^0 was observed more clearly to be one sharp peak (indicated by an arrow in Fig. 4(b)) with an appreciably large shift of the peak position for the VDF 65% samples annealed at 108–145°C. These two peaks were found to correspond to the two different phase transitions CL-to-HT and LT-to-HT [4,12,13] by measuring the temperature dependence of the X-ray diffraction, detailed results of which will be reported elsewhere. The shoulder observed for the VDF 73% sample may also correspond to the CL-to-HT phase transition, although it is not as clear as in the VDF 65% case because of the lower content of the CL phase in the VDF 73% sample.

The temperatures of the DSC peaks obtained from Fig. 4(a) and 4(b) are plotted as a function of the annealing temperature in Fig. 5 (a) and 5(b), respectively, for the VDF 73% and 65% samples. The thermal behavior of these samples may be classified into types A, B and C, which correspond, respectively, to the three parts of the DSC thermograms measured for the as-drawn and unannealed samples (upper curves in Fig. 5). The region A is

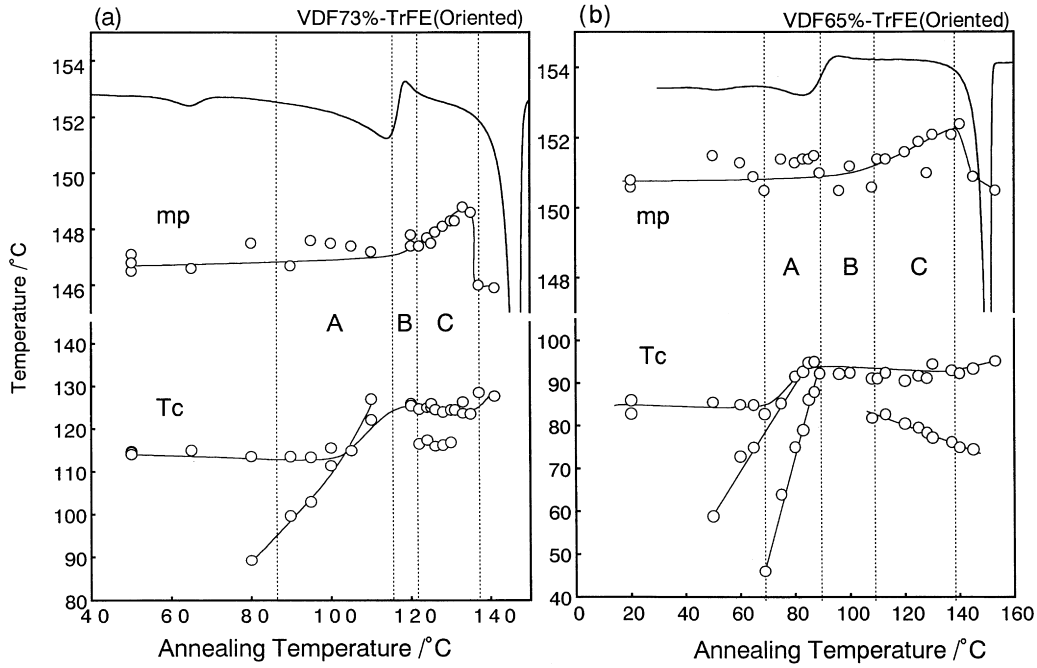

Fig. 5. Plots of the melting and transition points against the annealing temperature measured for the oriented VDF (a) 73% and (b) 65% samples. The DSC curves shown in the upper parts of these figures are those of the unannealed sample for reference purposes.

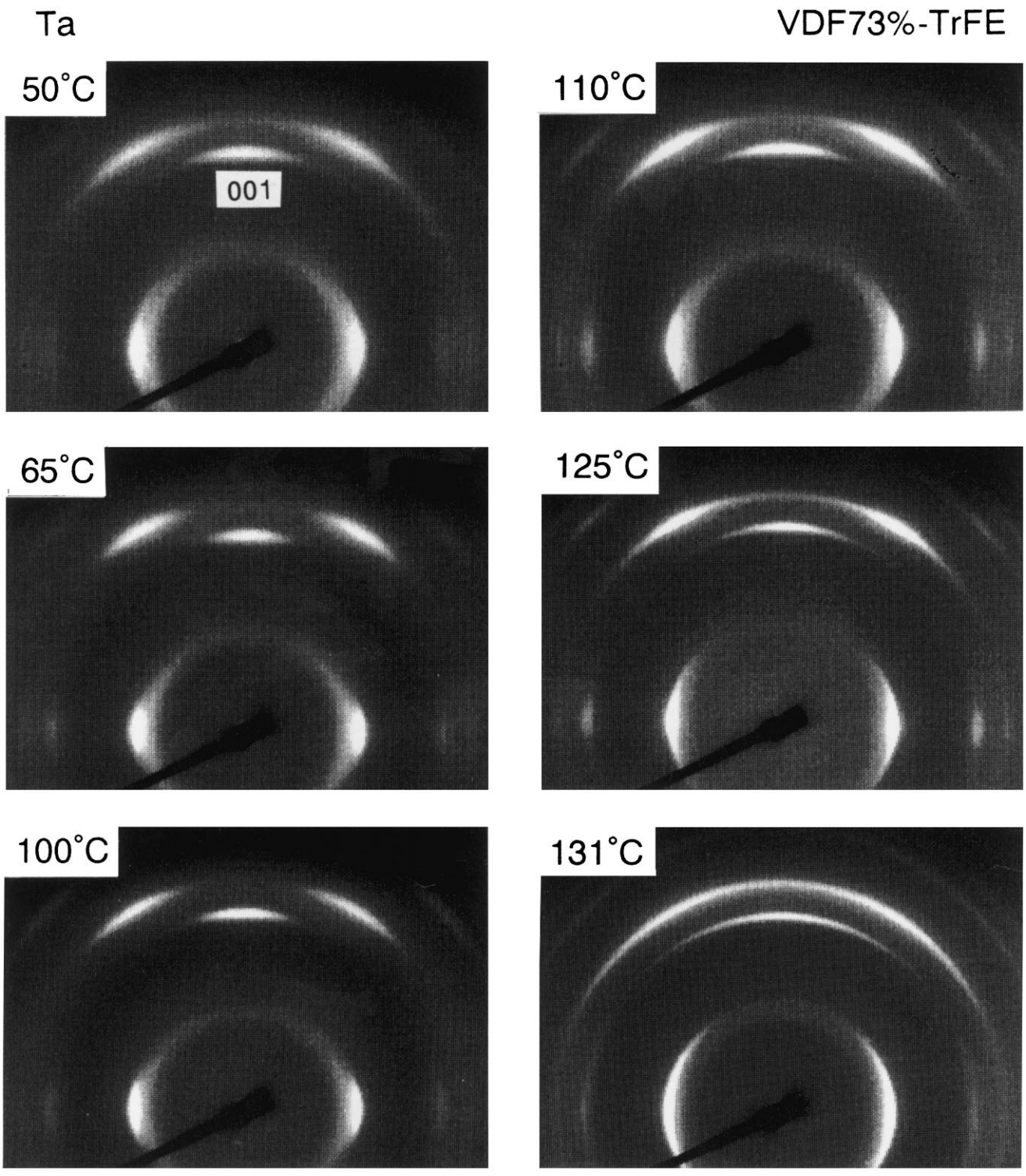

Fig. 6. Annealing temperature dependence of the X-ray fiber pattern of the uniaxially oriented VDF 73% copolymer samples measured at room temperature.

below the endothermic peak (around T_c^0), the region B covers the exothermic peak (around T_{exo}), and the region C is between the T_{exo} and the m.p. (or the temperature range of the HT phase). In a previous paper [24] the regions were roughly divided into two, but the present classification into the three regions is considered more reasonable and precise judging from the DSC curves. In region A, as the annealing temperature increases, the several endothermic peaks observed in Fig. 4 shift to the higher temperature side, and change into a single peak in region B. For the samples annealed in regions A and B, the melting point (m.p.) remains almost constant. When the sample is

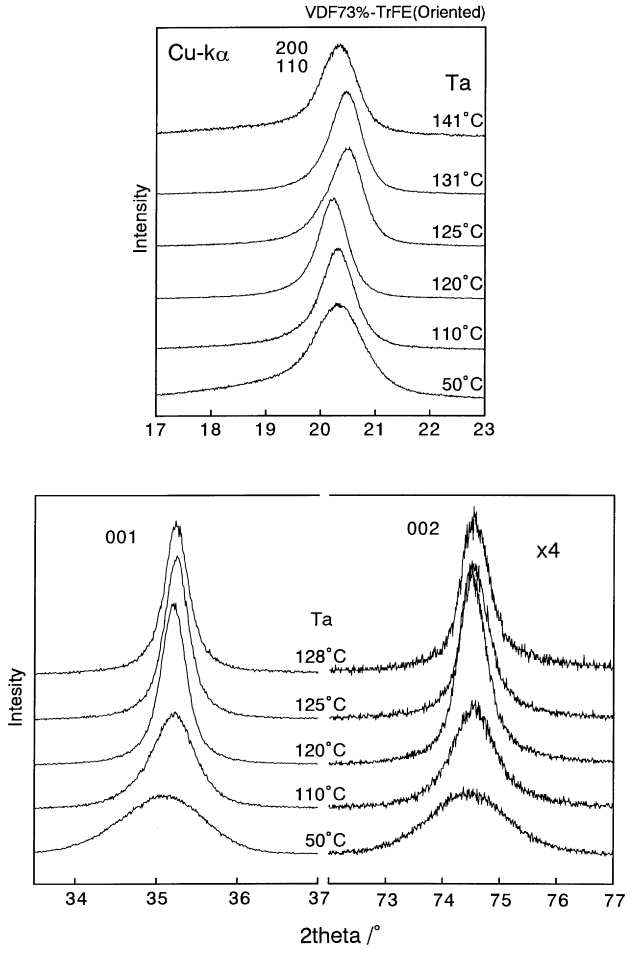

Fig. 7. X-ray diffraction profiles of the (200,110) and (00l) reflections measured at room temperature for the VDF 73% copolymer samples annealed at various temperatures. The incident X-ray beam is the Cu Kα line ($\lambda = 1.5418$ Å).

annealed in region C, a shoulder (for VDF 73%) or a sharp endothermic peak (for VDF 65%), indicated by arrows in Fig. 4, shift toward the lower temperature side. At the same time, the m.p. shifts to a higher position.

3.2. Annealing effect on the domain size

The annealing treatment induces changes in the crystallite size and inner structure of the crystal lattice. In order to investigate the crystalline state at room temperature for the samples annealed at various temperatures, X-ray fiber patterns were measured.

3.2.1. VDF 73% copolymer

Fig. 6 shows the annealing temperature dependence of the X-ray fiber pattern measured for the uniaxially oriented VDF 73% samples using an imaging plate system. As the annealing temperature increases, the reflections become

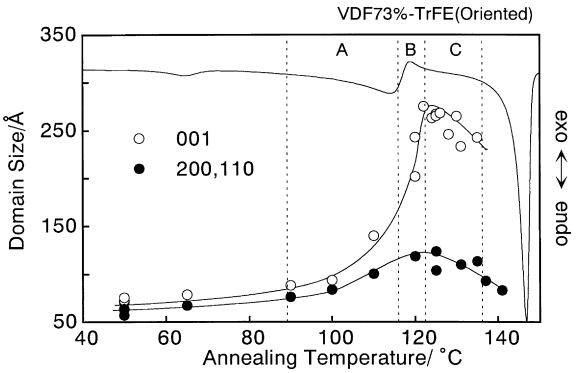

Fig. 8. Annealing effect on the domain size of the crystallite along the chain axis and in the lateral directions measured for the uniaxially oriented VDF 73% copolymer samples. The DSC curve for the unannealed sample is also shown for reference purposes.

sharper, although the degree of chain orientation becomes lower when the sample is annealed at a high temperature, such as 131°C. In the previous paper [24] we proposed experimentally the existence of domain structure in crystalline lamellae of VDF–TrFE copolymers. We evaluated quantitatively the sizes of the crystallite domain in the lateral direction as well as along the chain direction by measuring the half-width of the X-ray reflections. In Fig. 7 are reproduced X-ray profiles of the equatorial (200,110) and meridional (001) and (002) reflections, where the profiles were obtained by integration of the reflections in Fig. 6 along the azimuthal direction. The meridional reflection 001 becomes sharper as the annealing temperature increases, whereas the equatorial reflection does not change as much. The domain sizes were evaluated on the basis of Scherrer's Eq. (1). Fig. 8 shows the dependence of the domain sizes thus estimated on the annealing temperature. The domain sizes in both directions begin to increase when the samples are annealed in temperature region A (around 90 to 115°C). In region B (around 115 to 125°C), the sizes increase more rapidly: the increase rate along the chain axis is much higher than in the lateral direction. When the sample is annealed in region C (around 125 to 140°C), the domain sizes decrease only rather slightly.

The behavior of the domain size shown in Fig. 8 corresponds well to the change in the transition temperature and melting point seen in Fig. 5(a). In regions A and B, the domain size increases, and as a result the T_c shifts toward the higher temperature side, while in region C the domain size decreases and the DSC peak, indicated by an arrow in Fig. 4, shifts toward the lower temperature side. The origin of this correlation will be discussed later.

3.2.2. VDF 65% copolymer

In the case of the VDF 65% copolymer, as shown in Fig. 9, the X-ray diagram obtained for samples annealed above

Fig. 9. Annealing temperature dependence of the X-ray fiber pattern of the uniaxially oriented VDF 65% copolymer samples measured at room temperature.

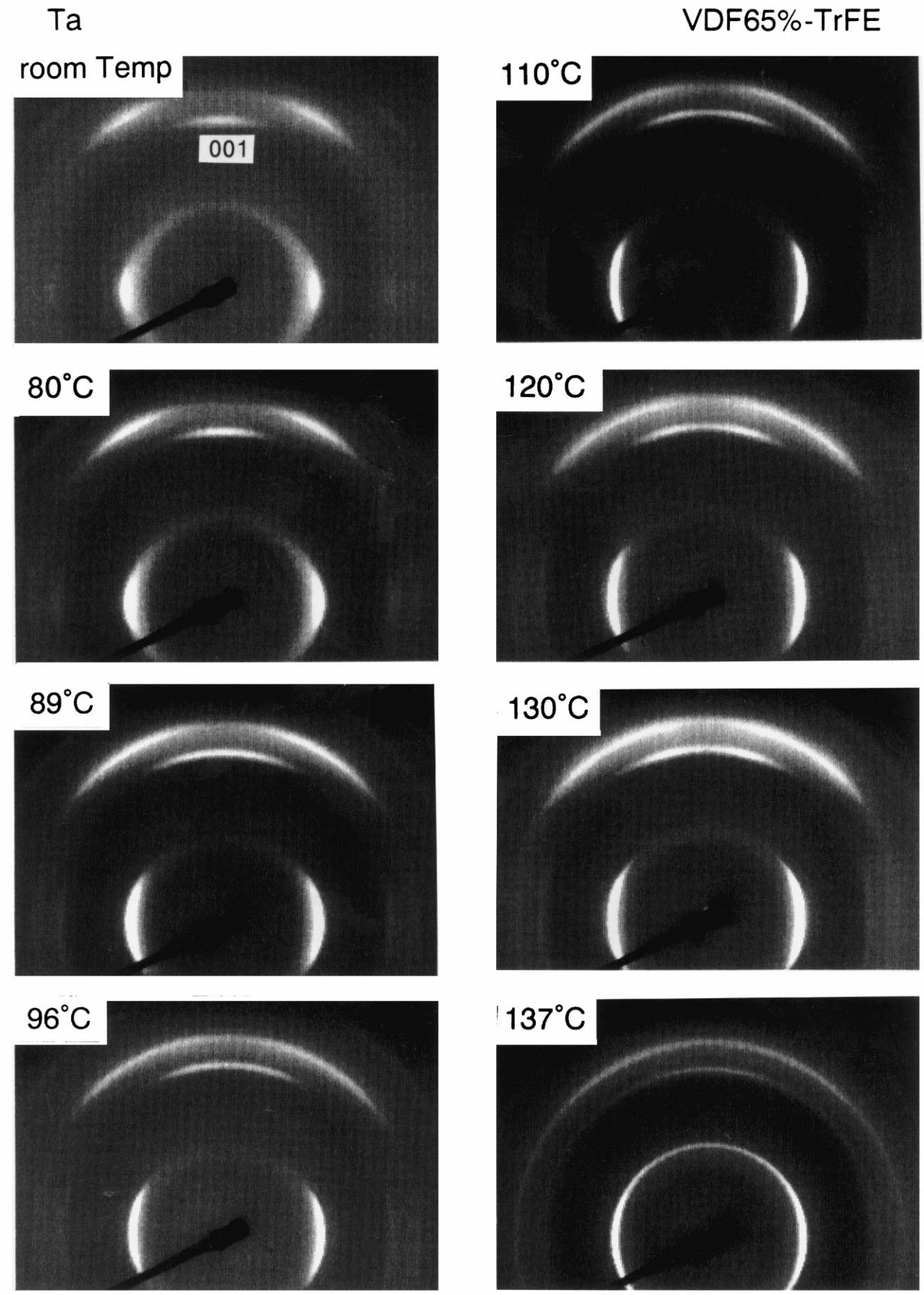
Ta
VDF65%-TrFE
room Temp
001
110°C
80°C
120°C
89°C
130°C
96°C
137°C

T_c (in regions B and C) shows a so-called tilting phenomenon of the crystallites: the reflection positions of the equatorial and layer lines shift up or down from the original horizontal lines (see the 110° fiber diagram, for example). This phenomenon was not detected for the VDF 73% samples. This tilting phenomenon is observed when the contribution of the CL phase becomes non-negligible. In the case of VDF 65% samples, the X-ray patterns are no longer those of the pure LT phase, but are those of mixtures of the LT and CL phases [4,12,13].

Fig. 10 shows the X-ray reflection profile in the equatorial and meridional directions measured for VDF 65% samples annealed at various temperatures, where the X-ray patterns were measured by using an Mo Kα line as the incident X-ray beam. Fig. 11 shows the domain size estimated from the half-width of the profiles shown in Fig. 10. The increasing domain size tendency is similar to that for the VDF 73% sample, shown in Fig. 8. In region B, however, the rate of increase of the domain size is not as drastic as that observed for the VDF 73% sample. As already pointed out in Fig. 9, a tilting phenomenon of the crystallites is observed in this annealing region for the VDF 65% samples containing both LT and CL phases. The domain size evaluated for the samples in region B may only be apparent. The small domain size in this region may be related to the existence of the CL phase. Because of the disordered structural feature of the CL phase, the X-ray reflections are broad on the whole. Therefore, in order to estimate the domain size exactly, we have to separate the reflection width into two components: one originating from the finite domain size and the other from the structure disorder. Since the profiles are quite complicated, it is very difficult to carry out this process at the present stage. Anyway, the origin of the characteristic behavior of the VDF 65% sample, which is different from that of the VDF 73% sample, is considered to be related to the generation of the CL phase from the LT phase, as already reported in previous papers [4,12,13].

3.3. FT-Raman spectral measurement

In this way, a close correlation between the T_c and the domain size was found by combining DSC and X-ray diffraction data. In order to investigate the annealing effect on the conformation of the molecular chains in the crystalline domains during heat treatment, the FT-Raman spectra were measured for the various samples used in the X-ray diffraction measurements. Fig. 12(a) and 12(b) show the FT-Raman spectra obtained in the frequency region 750–1500 cm^{-1} measured at room temperature for the annealed VDF 73% and 65% samples, respectively. The Raman bands of the VDF copolymers can be assigned to the vibrational modes of various types of chain conformations [4]. For example, the Raman band at 1289 cm^{-1} corresponds to the C–F stretching mode of the VDF trans sequence longer than TTTT, the band at 842 cm^{-1} to the VDF trans sequence longer than TTT, and the 811 cm^{-1} band to the gauche form and the amorphous phase. In order to estimate the integrated intensities of these key bands, overlapped bands were sepa-

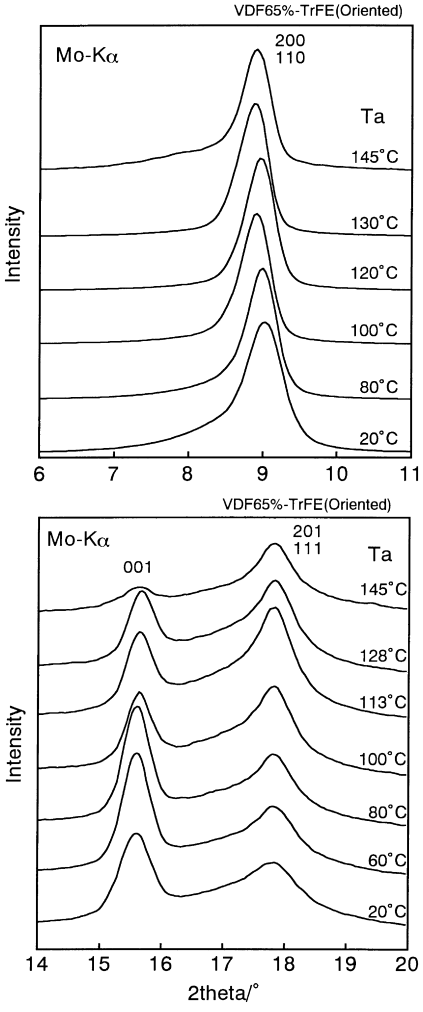

Fig. 10. X-ray diffraction profiles of the (200,110) and (001) reflections measured at room temperature for the VDF 65% copolymer samples annealed at various temperatures. The incident X-ray beam is the Mo Kα line (λ = 0.71073 Å).

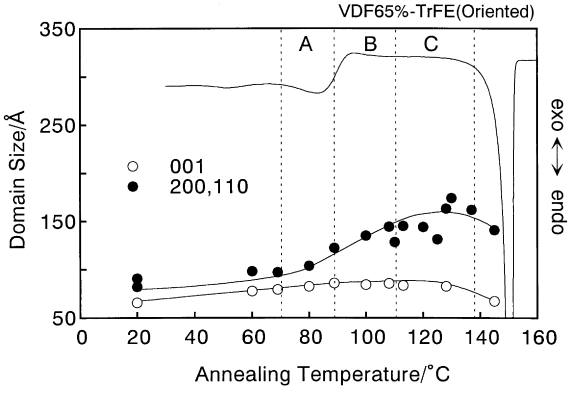

Fig. 11. Annealing effect on the domain size of the crystallite along the chain axis and in the lateral directions measured for the uniaxially oriented VDF 65% copolymer samples. The DSC curve for the unannealed sample is also shown for reference purposes.

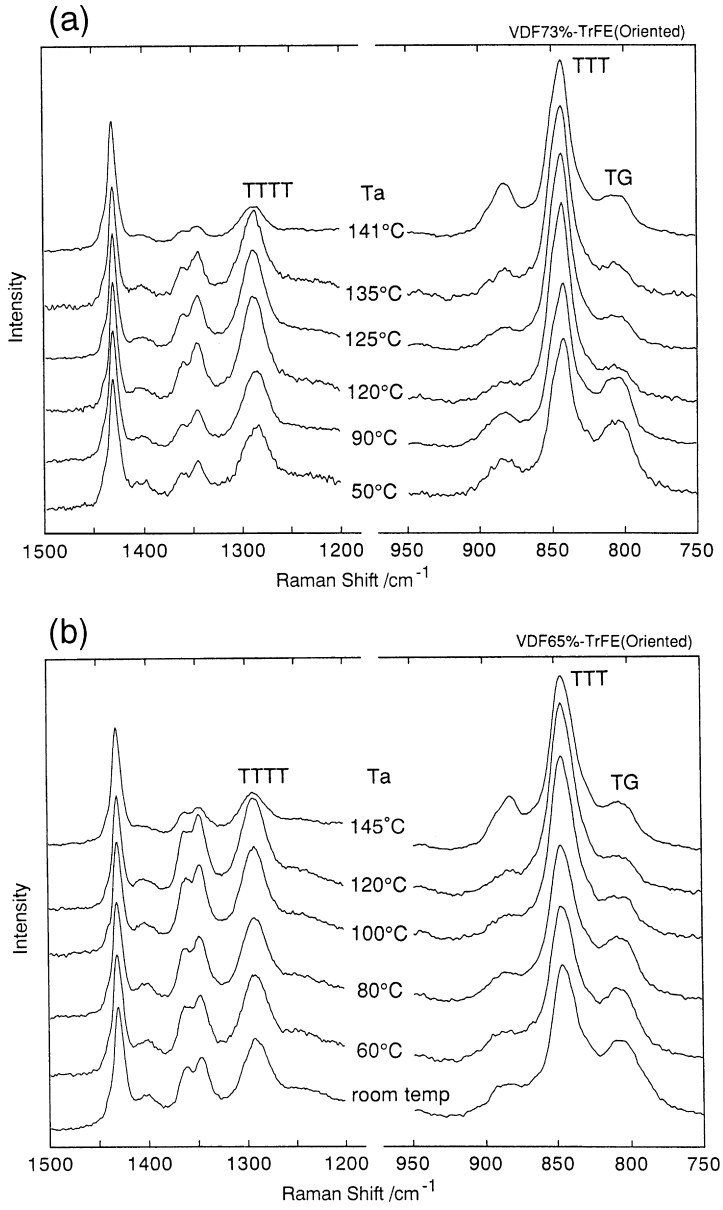

Fig. 12. Raman spectra measured at room temperature for the uniaxially oriented VDF (a) 73% and (b) 65% copolymer samples annealed at various temperatures.

rated into their components by a curve fitting technique. In Fig. 13, Raman band intensities are plotted against the annealing temperature. When the sample is annealed in region A, the bands of the long trans sequences at 1289 cm^{-1} (TTTT, solid circle) and 842 cm^{-1} (TTT, empty circle) increase in intensity, and the gauche and amorphous bands at 811 cm^{-1} correspondingly decrease. In region B, the band of the TTT sequence still increases in intensity, but the band of the longer trans sequence (TTTT) reduces the increasing rate of the intensity. In region C, the TTT band keeps the intensity almost constant but the TTTT band decreases the intensity gradually. When the annealing is carried out in the melting temperature region, the 1289 cm^{-1} band decreases in intensity drastically. This characteristic behavior could be observed almost commonly for both the VDF 73% and the VDF 65% samples, although the tendency is more marked for the VDF 73% samples.

3.4. Structural changes of domains

Fig. 14 illustrates schematically the structural change in the domains, which could be deduced from all the experimental data presented above. The crystalline lamellae of the as-drawn unannealed sample are considered to consist of small domains, represented by cylinders, where the arrows show the CF_2 dipole moments of the planar zigzag chains which orient randomly among the domains (see Fig. 2).

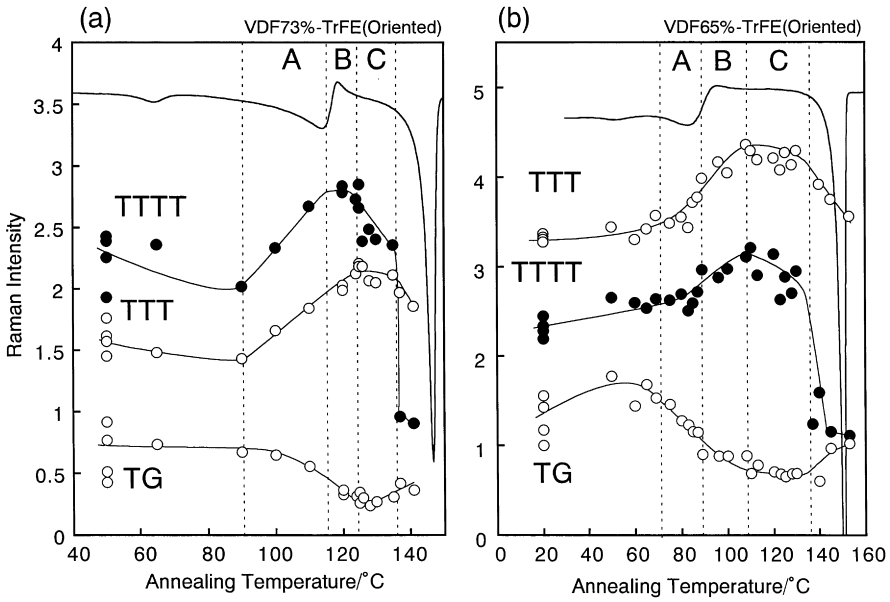

Fig. 13. Annealing effect on the integrated intensities of the Raman bands characteristic of the various conformations evaluated for the uniaxially oriented VDF (a) 73% and (b) 65% copolymer samples. The DSC curves for the unannealed samples are shown for reference purposes.

These domains are assumed to give rise to X-ray scattering incoherently from one another. In other words, the half-width of the X-ray reflection is related to the size of an individual domain.

3.4.1. VDF 73% copolymer

In the case of the VDF 73% samples, when annealed in regions A and B, the crystallite length along the *c* axis increases drastically, having originated from the large growth of the trans zigzag chain segments. In region C, as deduced from a decrease in the Raman band intensity of the TTTT segment, the long trans sequence is cut short by an invasion of gauche conformational defects. This is reasonable because region C corresponds to the temperature region of the HT phase and some gauche bonds generated in this region may be trapped in the molecular chains even after the sample is quenched to room temperature. This irregular gauche contamination may cause the shift to lower temperature of the DSC peak observed in region C.

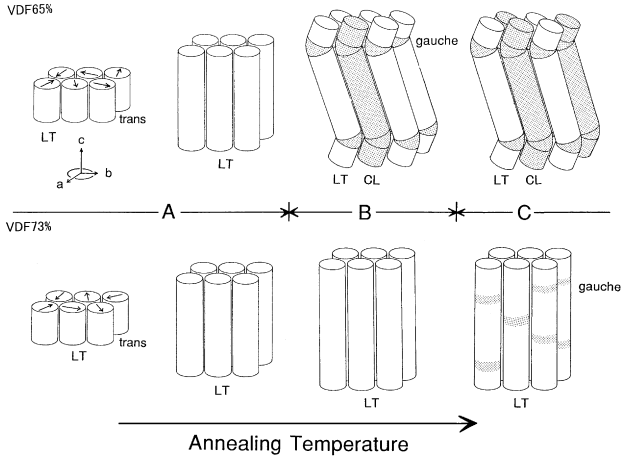

Fig. 14. An illustration of the change in the domain structure caused by heat treatment of the VDF 73% and 65% copolymers.

3.4.2. VDF 65% copolymer

In this case, the domain size grows in region A similarly to the case of VDF 73%. However, as the sample is annealed in the B and C regions, the pure LT phase transforms to a mixture of the CL and LT phases and the growth of the domain is apparently halted. At the same time, a tilting phenomenon occurs due to an invasion of gauche defects into the trans segments, as shown in Fig. 14. When the sample is heated, the LT and CL phases transform to the HT phase in a different manner, giving two different DSC curves as already indicated in Fig. 4(b). As will be reported elsewhere, the endothermic peak at the lower temperature side in Fig. 4(b) (indicated by an arrow) corresponds to the transition from the CL to the HT phase. This transition peak shifts to the lower temperature side as the annealing temperature is increased. The gauche bonds included in the CL phase may play a role as nucleation agent for a conformational transition from the trans to the gauche form; in other words, transformation from the CL to the HT phases is considered to occur easily. Annealing at higher temperature induces an increment in the gauche content, resulting in a lower shift of the T_c, as seen in Fig. 4(b).

4. Conclusions

In this paper, we investigated the effect of annealing on the structures and transition temperatures of the VDF 73%

and 65% samples. For both samples, the transition temperature increased when the samples were annealed in the ferroelectric–paraelectric phase transition region. The domain size, evaluated from the integrated width of the X-ray reflections, increased drastically at these annealing temperatures. As the annealing temperature was increased further (region C for the VDF 73% sample and region B for the VDF 65% sample), the transition temperature decreased markedly. At this time, the domain size decreased slightly and the trans sequential length of the molecular chains decreased due to an invasion of gauche bond defects. A characteristic of the VDF 65% sample was that the annealing in temperature region B induced a tilting phenomenon of trans zigzag chains in the crystalline region. The phenomenon was not actually detected for the VDF 73% sample. This difference may arise from the difference in the sequential lengths of regular VDF monomeric units of these two samples [13].

In order to ascertain the origins of these annealing effects more clearly, we have to clarify the structural changes occurring 'during' heat treatment at high temperatures. The experimental data collected for this purpose will be reported in the near future.

Acknowledgements

We would like to express our gratitude to Daikin Kogyo Co. Ltd., Japan, for supplying the VDF–TrFE copolymer samples.

References

[1] Furukawa T, Date M, Fukada E, Tajitsu Y, Chiba A. Jpn J Appl Phys 1980;19:L109.
[2] Fukada E. Phase Transitions 1989;18:135.
[3] Furukawa T. Phase Transitions 1989;18:143.
[4] Tashiro K. In: Nalwa HS, editor. Ferroelectric polymers. New York: Marcel Dekker, 1995: chapter 2.
[5] Yamada T, Ueda T, Kitayama T. J Appl Phys 1981;52:948.
[6] Higashibata Y, Sako J, Yagi T. Ferroelectrics 1981;32:85.
[7] Tashiro K, Takano K, Kobayashi M, Chatani Y, Tadokoro H. Polymer Commun 1981;22:1312.
[8] Lovinger AJ, Davis GT, Furukawa T, Broadhurst MG. Macromolecules 1982;15:323.
[9] Davis GT, Furukawa T, Lovinger AJ, Broadhurst MG. Macromolecules 1982;15:329.
[10] Lovinger AJ, Furukawa T, Davis GT, Broadhurst MG. Polymer 1983;24:1225.
[11] Lovinger AJ, Furukawa T, Davis GT, Broadhurst MG. Polymer 1983;24:1233.
[12] Tashiro K, Takano K, Kobayashi M, Chatani Y, Tadokoro H. Polymer 1984;25:195.
[13] Tashiro K, Takano K, Kobayashi M, Chatani Y, Tadokoro H. Ferroelectrics 1984;57:297.
[14] Tashiro K, Kobayashi M. Polymer 1988;29:4429.
[15] Green JS, Rabe JP, Rabolt JF. Macromolecules 1986;19:1725.
[16] Ishii F, Odajima A, Ohigashi H. Polym J 1983;15:875.
[17] McBrierty VJ, Douglass DC, Furukawa T. Macromolecules 1982;15:1063.
[18] McBrierty VJ, Douglass DC, Furukawa T. Macromolecules 1984;17:1136.
[19] Ishii F, Odajima A. Polym J 1986;18:539.
[20] Ishii F, Odajima A. Polym J 1986;18:547.
[21] Legrand JF. Ferroelectrics 1989;91:303.
[22] Legrand JF, Frick B, Meurer B, Schmidt VH, Bee M, Lajzerowicz J. Ferroelectrics 1990;109:321.
[23] Li GR, Kagami N, Ohigashi H. J Appl Phys 1992;72:1056.
[24] Tashiro K, Tanaka R, Ushitora K, Kobayashi M. Ferroelectrics 1995;171:145.
[25] Stack GM, Ting RY. J Polym Sci, Part B 1988;26:55.
[26] Kim KJ, Kim GB, Vanlencia CL, Rabolt JF. J Polym Sci, Part B 1994;32:2435.
[27] Gregorio jr R, Botta M. J Polym Sci Part B 1998;36:403.